Case Study 2

Detection of Oil Slicks using MODIS and SAR Imagery

Chuanmin Hu[*1], **Xiaofeng Li**[2], **William G. Pichel**[3]

2.1 Background

Oil pollution can cause extensive damage to marine and terrestrial ecosystems. Every year, huge quantities of oil and petroleum products enter the sea, land, and groundwater (NAS, 2003). The pollution can come from a variety of sources, including leakage from oil transportation, accidents on oil platforms, atmospheric deposition, and seepage from natural seeps. Timely and accurate detection of oil pollution in the ocean can help management and research efforts, yet it is often a difficult task due to limited technical means in monitoring the vast ocean.

Remote sensing provides rapid, frequent, and synoptic measurement of the ocean's surface waters, and thus has been used widely to monitor oil pollution at sea, as well as in lakes. The remote sensing instruments include optical, microwave, and radar (e.g., synthetic aperture radar, SAR) sensors which can be equipped on both aircrafts and satellites. Each of the instruments and measurement platforms has its own advantages and disadvantages (Fingas and Brown, 1997; 2000; Brekke and Solberg, 2005). While airborne remote sensing offers the highest resolution (i.e., the sharpest image) and fastest response to a pollution event, it is often too expensive to be used for operational monitoring. In contrast, satellite remote sensing provides more frequent measurements of the ocean, hence more suitable for oil pollution monitoring.

Among the various satellite instruments, SAR is perhaps the most often used for oil detection at sea. The sea-surface backscattered radar signal is modulated by the wind-induced capillary waves, and thus carries information on the surface roughness. An ocean surface oil film has higher surface tension than water, and can dampen the surface capillary waves, resulting in a smoother sea surface. This in

[1]College of Marine Science, University of South Florida, 140 7th Ave., S., St. Petersburg, FL 33701, USA. *Email address: hu@marine.usf.edu
[2]IMSG, NOAA NESDIS, USA
[3]NOAA NESDIS, USA

turn reduces the backscattered radar signal, making oil contaminated areas appear as dark patches in SAR images.

Because radar signals can "penetrate" clouds, SAR images are cloud free and efficient for detecting the various ocean surface features. However, routine application of SAR data is limited by its high-cost and narrow satellite swath (i.e., spatial and temporal coverage). Depending on the measurement mode, measurement of the same place can require days to weeks. These factors make it desirable to seek alternatives to complement SAR observations.

There are currently several Sun-synchronous, polar-orbiting satellite ocean-colour instruments that can measure the ocean's bio-optical properties every day. These include the Sea-viewing Wide Field-of-view Sensor (SeaWiFS, 1997 - present; McClain et al., 2004), the MODerate resolution Imaging Spectroradiometer (MODIS, 1999 - present for Terra, and 2002 - present for Aqua; Esaias et al., 1998), and the Medium Resolution Imaging Spectrometer (MERIS, 2002 - present). While MERIS was launched by the European Space Agency (ESA), SeaWiFS and MODIS are supported by the U.S. NASA. Global data are available for free downloading in near real-time. In particular, MODIS is equipped with several 250-m and 500-m resolution bands, representing a significant enhancement over the present coastal observation capability for the international community. The combined MODIS-Terra and MODIS-Aqua missions cover the global ocean in any single day, thus providing great potential to develop ocean applications.

Hu et al. (2003) used MODIS 250-m resolution data to detect and monitor oil spills in a turbid lake in Venezuela. After removing clouds, two images per week were obtained at no cost. The detection was possible because the high turbidity of the lake water provided a "bright" background where the highly light-absorbing oil films could be visualized. In the oligotrophic ocean, the water background is also dark, making oil detection difficult. However, Hu et al. (2009) showed that when MODIS imagery contained sun glint (i.e., specular reflection of the solar beam), high contrast was found between oil slicks and the background water. The contrast is not due to the difference in optical properties of the oil film and the water (as evidenced by the lack of contrast in other glint-free images), but due to the oil-modulation of the surface capillary waves - the same principle for SAR measurements. Indeed, the ability of visible imagery (including those from space shuttle photos) over sun glint regions to serve as effective radar signals was recognized decades ago and demonstrated recently using satellite imagery (Chust and Sagarminaga, 2007). However, its routine application has been difficult due to lack of near-daily data. The free availability of MODIS daily data for the global oceans makes it possible to implement a cost-effective means for oil spill monitoring.

Here, using MODIS 250-m resolution imagery and RADARSAT-1 SAR 25-m resolution imagery, we show several examples of how oil slicks are identified and interpreted. Three case studies are presented here. The first covers the western Gulf of Mexico (GOM, 18° – 31°N, 98° – 81°W) where numerous oil seeps exist. The

second covers the NE GOM where a tragic oil spill event began on 20 April 2010. The last example covers the East China Sea (ECS, 25° – 35°N, 120° – 130°E) where oil pollution from terrestrial and ship discharges is well known.

2.1.1 Data Source and Processing Methods

SAR data from RADARSAT-1 (C-band radar with horizontal polarization and 100-km swath width) were obtained during the Alaska SAR Demonstration (AKDEMO) project. These 25-m resolution images were standard beam mode scenes, processed at the Alaska Satellite Facility (ASF) at the University of Alaska, Fairbanks. The images provided relative intensity of the SAR signal (in digital numbers), and were navigated and analyzed using the software ENVI (Environment for Visualizing Images, version 4.2). The geo-referenced (or map-projected) digital images were stored in PNG graphical format.

All MODIS data were downloaded from the NASA Goddard Space Flight Center (GSFC) at no cost (http://oceancolor.gsfc.nasa.gov). These data are open to the public in near real-time and do not require data subscription. The following steps were used to generate geo-referenced MODIS images at 250-m resolution.

1. MODIS Level-0, 5-minute granules, were downloaded from NASA/GSFC;
2. MODIS Level-0 data were processed to generate Level-1b (calibrated total radiance) data for the 36 spectral bands using the SeaWiFS Data Analysis System (SeaDAS version 5.1). The Level-1b data were stored in computer files in HDF (Hierarchical Data Format);
3. MODIS Level-1b data were corrected for gaseous absorption (ozone and other gases) and Rayleigh scattering effects, resulting in the Rayleigh-corrected reflectance:

$$R_{rc,\lambda}(\theta_0, \theta, \Delta\phi) = \pi L_{t,\lambda}{}^*(\theta_0, \theta, \Delta\phi)/(F_0\lambda) \times \cos\theta_0) - R_{r,\lambda}(\theta_0, \theta, \Delta\phi) \quad (2.1)$$

   where λ is the wavelength for the MODIS band, $L_t{}^*$ is the calibrated sensor radiance after correction for gaseous absorption, F_0 is the extraterrestrial solar irradiance, θ_0 is the solar zenith angle, θ is the sensor (viewing) zenith angle, $\Delta\phi$ is the relative azimuth between the sun and the satellite, and R_r is the reflectance due to Rayleigh (molecular) scattering. The solar-viewing geometry is defined by $(\theta_0, \theta, \Delta\phi)$, which changes from pixel to pixel. This step used the software CREFL from the University of Wisconsin (Liam Gumley). The R_{rc} data of 7 MODIS bands (469, 555, 645, 859, 1240, 1640, and 2130 nm) were stored in HDF computer files. Figures 2.1a and b show examples of the R_{rc} Red-Green-Blue images using 645, 555, and 469-nm as R, G, and B, respectively. If two consecutive 5-minute granules were required to cover the study region, the Level-0 data were combined together before Step 2 was performed;
4. The R_{rc} data were geo-referenced to a cylindrical/equidistance (rectangular or geographic lat/lon) projection for the area of interest, defined by the

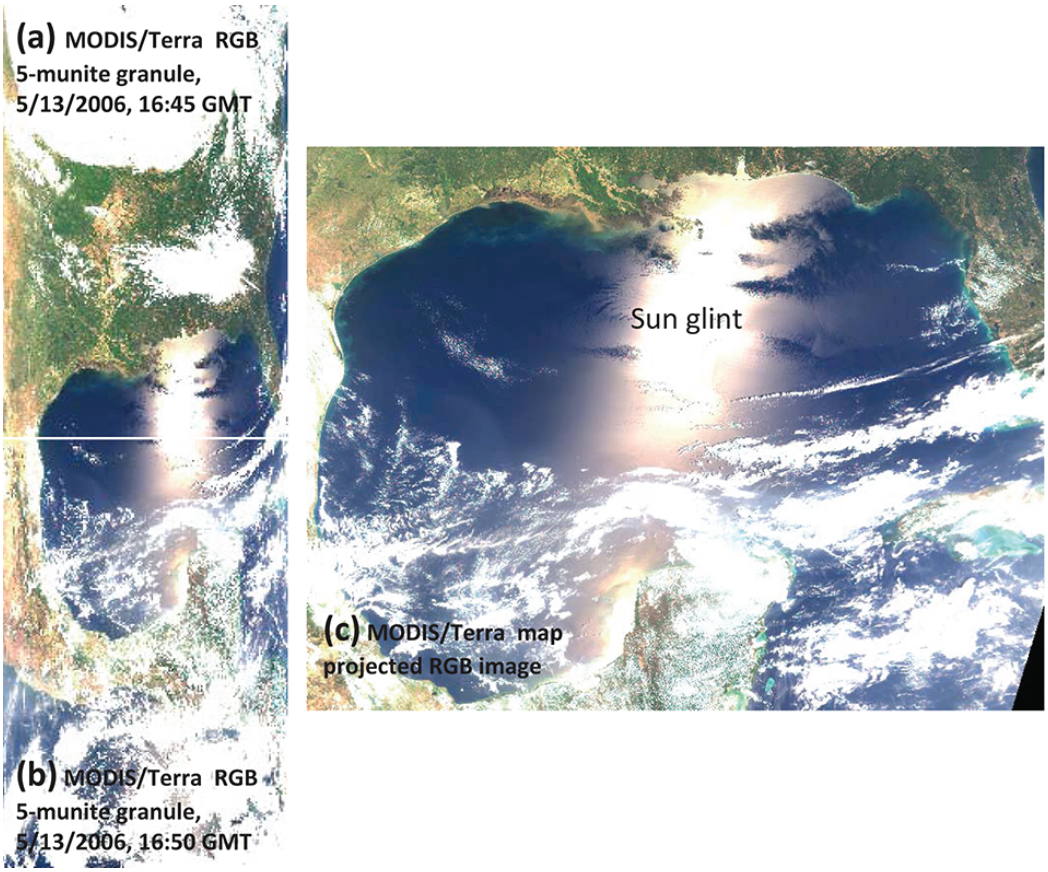

Figure 2.1 Map projection of the MODIS Level-1b R_{rc} data. (a) and (b): two consecutive MODIS/Terra 5-minute granules on 13 May 2006. Each granule contains R_{rc} data at 645 and 859 nm with a dimension of 5416 x 8120, and R_{rc} data from other bands (469, 555, 1240, 1640, and 2130 nm) with a dimension of 2708 x 4060. The RGB images were composed of R_{rc} at 645 (R), 555 (G), and 469 nm (B). (c): rectangular projection of the two granules to cover the area of interest (Gulf of Mexico, from 18° to 31°N and 98° to 81°W). There are 440 image pixels per degree, corresponding to about 250-m per pixel.

North-South and East-West bounds. Because 1 degree is about 110 km, the map-projected data have 440 image pixels per degree, corresponding to 250 m per image pixel. Although only the MODIS 645- and 859-nm bands have a nadir resolution of 250 m, other bands at 500-m resolution were interpolated to 250-m resolution using a sharpening scheme similar to that for Landsat. The mapping software was written in-house using C++ and PDL (Perl Data Language) with an accuracy of about 0.5 image pixel;

5. The map projected R_{rc} data at 645, 555, and 469 nm were converted to byte values using a linear stretch (coefficients determined by trial-and-error), and then used as the red, green, and blue (RGB) channels, respectively, to compose a RGB image. Figures 2.1c shows the map projected RGB image at 250-m

resolution from the combined 5-minute granules in Figures 2.1a and b;

6. The RGB image was loaded in the software ENVI for display and analysis.

2.2 Demonstration

Because of the synoptic coverage (often >10 degrees in both N-S and E-W directions) and medium resolution (250-m per pixel), the MODIS RGB image is very large (e.g., the dimension of Figure 2.1c is 7480 × 5720 pixels). Further, the colour stretch is compromised to cover both sensitivity (the smallest difference between pixels) and dynamic range (the lowest and highest pixel values). Thus, interactive stretching and zooming functions are required to visualize the various image features. While several commercial software packages (e.g., ArcInfo or Erdas Imagine, or any other software that has basic image processing capabilities) can be used, we use the software ENVI to demonstrate how the oil-like features are identified.

First, the RGB image is loaded into ENVI by using the "File → Open Image File" function. Three display windows are shown (Figure 2.2 top panels): scroll, image, and zoom. The scroll window shows the entire region at reduced resolution to serve as a browse image; the image window shows a portion of the image at full resolution (250-m); and the zoom image enlarges a smaller portion by 4 times.

During the initial display in ENVI, the colours are stretched linearly from 0 to 255 to cover the entire image. This often makes the subtle surface features invisible. The image window is thus colour enhanced by a "Gaussian" enhancement, using the menu of "Image → Enhance → Gaussian". The result is that the image window is colour enhanced, at the price of either over-stretching or under-stretching for other regions. The various image panels in Figure 2.2 show the before-after comparison using the Gaussian enhancement.

What are the identified dark slicks in Figure 2.2? SAR data collected on the same day in an adjacent region showed identical features to those appearing in the corresponding MODIS image (Figure 2.3). Further, the MODIS image for the region in Figure 2.3 contains low to moderate sun glint (Hu et al., 2009), and another MODIS image collected 3 hours later over the same region, but without sun glint, shows no features at all. All this combined evidence suggests that these dark features are indeed due to dampened surface roughness and not due to changes in water's optical properties.

Several other processes, in addition to oil films, can lead to reduced surface roughness. These include phytoplankton or fish induced surface surfactant, shoals, and coastal freshwater jets (Alpers and Espedal, 2004). The region shown in Figure 2.3 is located in an oligotrophic ocean away from land, so these potential processes can be ruled out. The most striking evidence is that these features are recurrent in the same place, and they can also be observed in other images under optimal conditions (cloud free, with some degree of sun glint). Figure 2.4 shows two other

examples, both using ENVI's Gaussian enhancement, where the slicks from two different days appear to have a one-to-one relationship and originate from the same locations. They are oriented differently due to different surface currents and winds. The only explanation, then, is that these surface slicks are oil films from oil seeps on the ocean floor. Indeed, the NW GOM is well known to have numerous oil seeps and previous studies using a variety of methods (including remote sensing) confirmed the existence of oil seeps (McDonald et al., 1993; 1996). Thus, even without *in situ* validation, we can conclude that these surface features are indeed oil slicks floating on the surface.

This application is further demonstrated using MODIS imagery to examine a recent tragic oil spill event. On 20 April 2010, an explosion occurred on the oil drilling rig, the Deepwater Horizon, in the northern GOM (28.74°N, 88.37°W). After burning for a day, the rig sank to the 1500-m ocean floor, resulting in the largest oil spill event in the U.S. history. The main cause of the spill was a continuously leaking oil well, with estimates of at least 5,000 barrels per day (indeed, later estimates by several independent groups showed up to 50,000 barrels per day). Various methods have been used to assess the volume, fate, and trajectory of the spilled oil to help mitigate the potential adverse impacts on ocean and terrestrial ecosystems. Using the principles shown above, we processed and provided MODIS imagery in near real-time to the management agencies and researchers, and made them available online in Google-Earth compatible format to facilitate visualization and tracking of the spill (http://optics.marine.usf.edu/events/GOM_rigfire, Figure 2.5). In Figure 2.5b it can be seen that among the scattered clouds there is a suspicious feature. The feature appears like clouds, but its spectral shape is noticeably different from clouds, with relatively lower reflectance in the blue wavelengths due to enhanced Rayleigh scattering along the sun glint beam (the same principle behind why sunset is reddish). The sun glint reflectance and viewing angle (relative to the mirror direction of the sun) were estimated as 0.048 sr^{-1} and 12.6°, respectively. Further, the spatial shape and lack of shadow also indicate that the suspicious feature is oil. Figures 2.5c and d show two other examples from the same day from MODIS-Terra and MODIS-Aqua observations, respectively. Due to changes in the solar/viewing geometry, the same oil slicks show positive contrast in the morning but negative contrast in the afternoon, agreeing with what has been observed from natural oil slicks in the GOM (e.g., Figure 2.4).

Note that the reason for using RGB images instead of individual MODIS bands (e.g., 859 nm) is that clouds and cloud shadows can be easily visualized and ruled out as potential oil slicks.

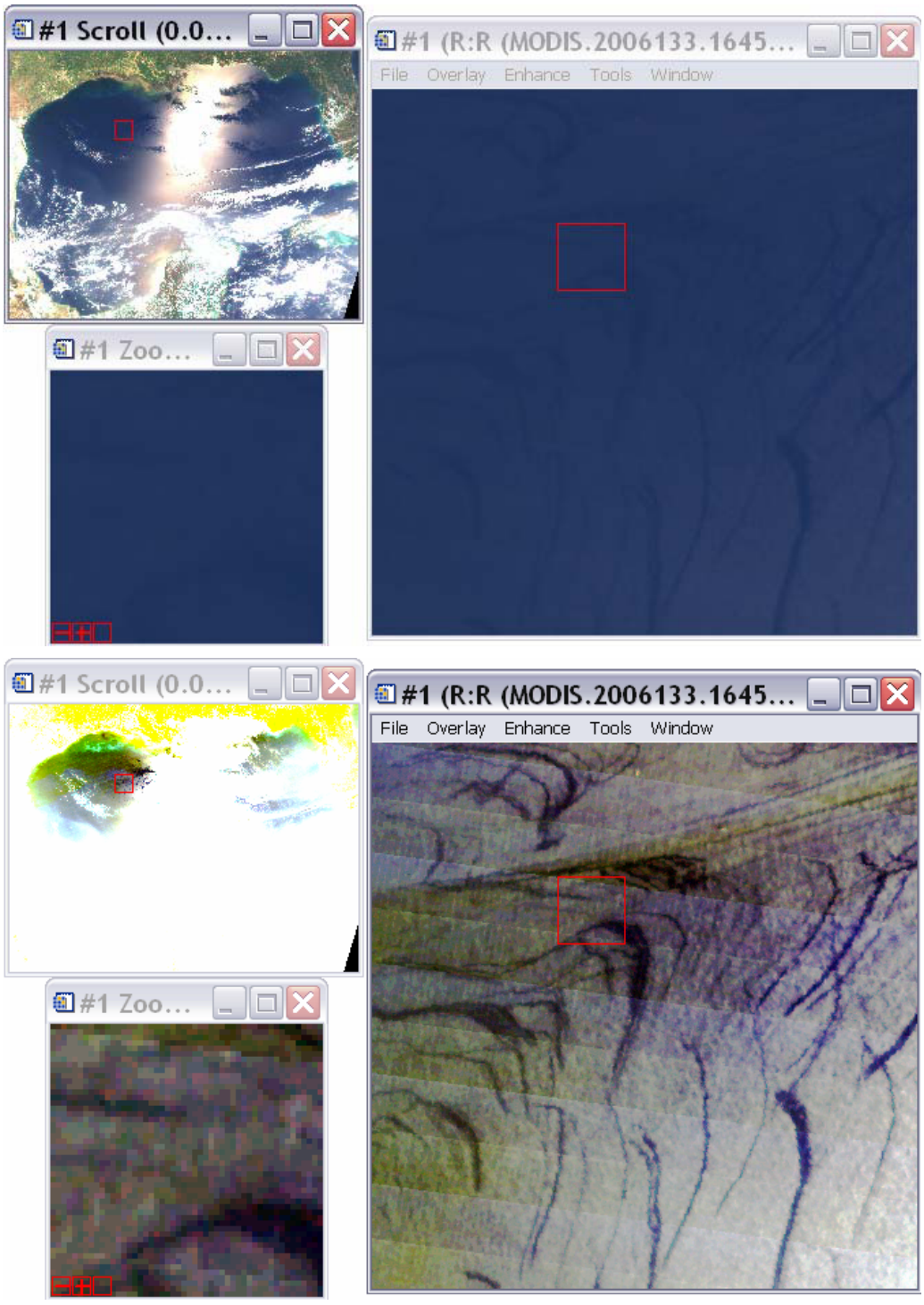

Figure 2.2 Interactive colour stretching within the software ENVI is used to enhance the contrast between the oil-like features and the background water. Top: original RGB image in scroll (upper left), image (upper right), and zoom (bottom left) display windows. Bottom: the same image after Gaussian enhancement. Similar enhancement can be performed in other software packages.

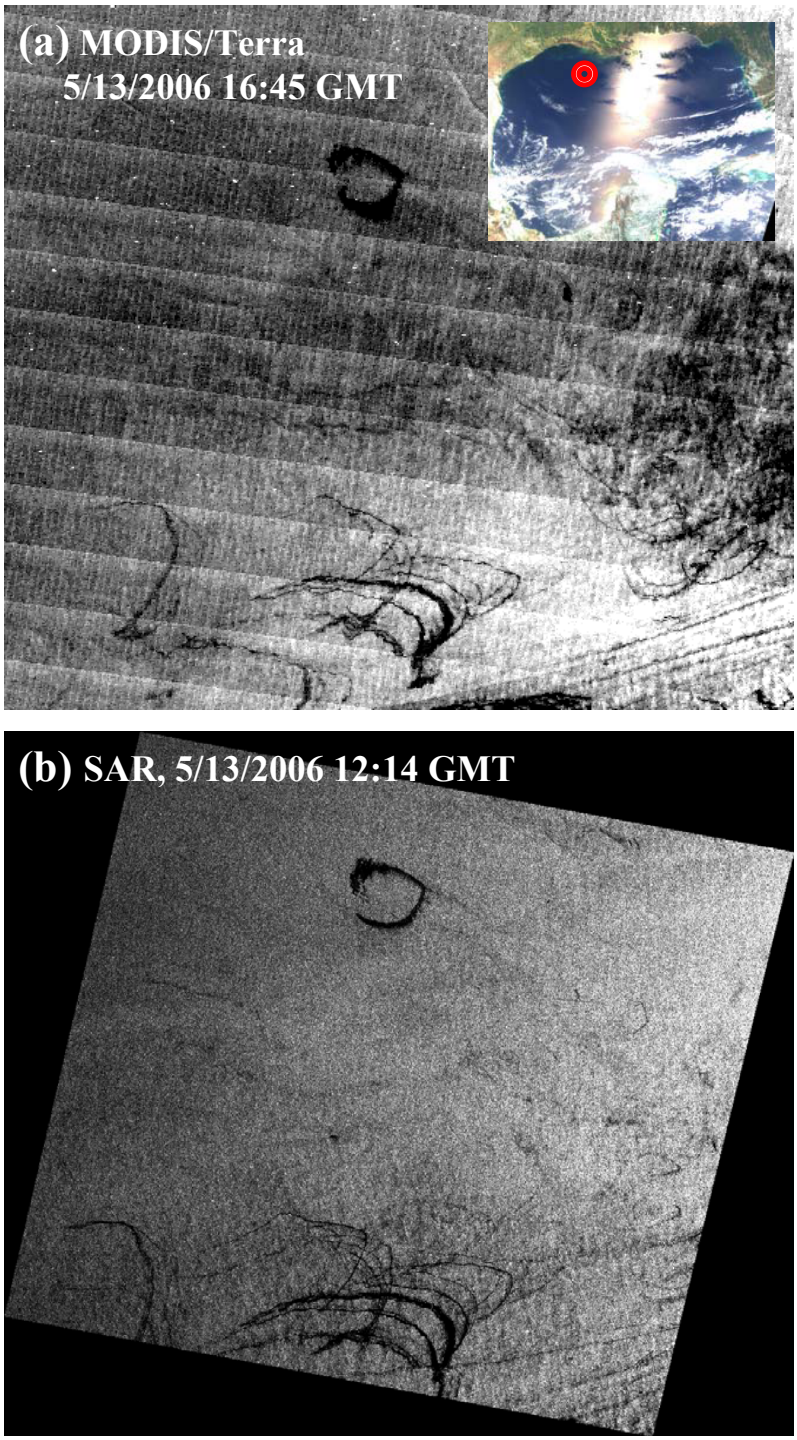

Figure 2.3 MODIS/Terra image (a) and SAR image (b) showing oil slicks in the NW Gulf of Mexico (inset MODIS Red-Green-Blue figure) between 27.38° to 28.48°N and 93.25° to 92.01°W. The data were collected 4.5 hours apart, yet the slick patterns appear identical. The MODIS image was coloured stretched in ENVI using Gaussian enhancement.

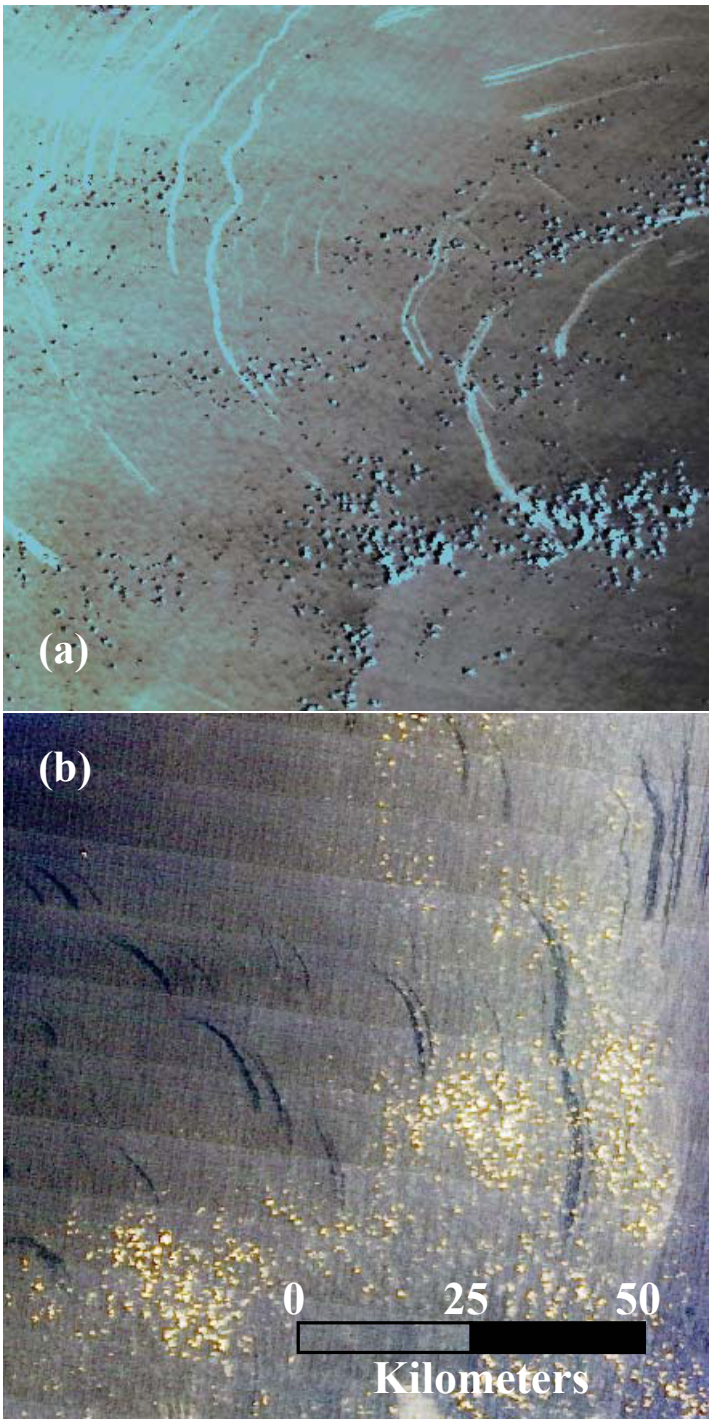

Figure 2.4 MODIS/Terra images collected on 5/13/2001 (a) and 5/24/2001 (b) showing oil slicks in the NW Gulf of Mexico as positive and negative contrasts, respectively, against the background. The contrast change is due to different solar/viewing geometry in the sun glint patterns (Hu et al., 2009).

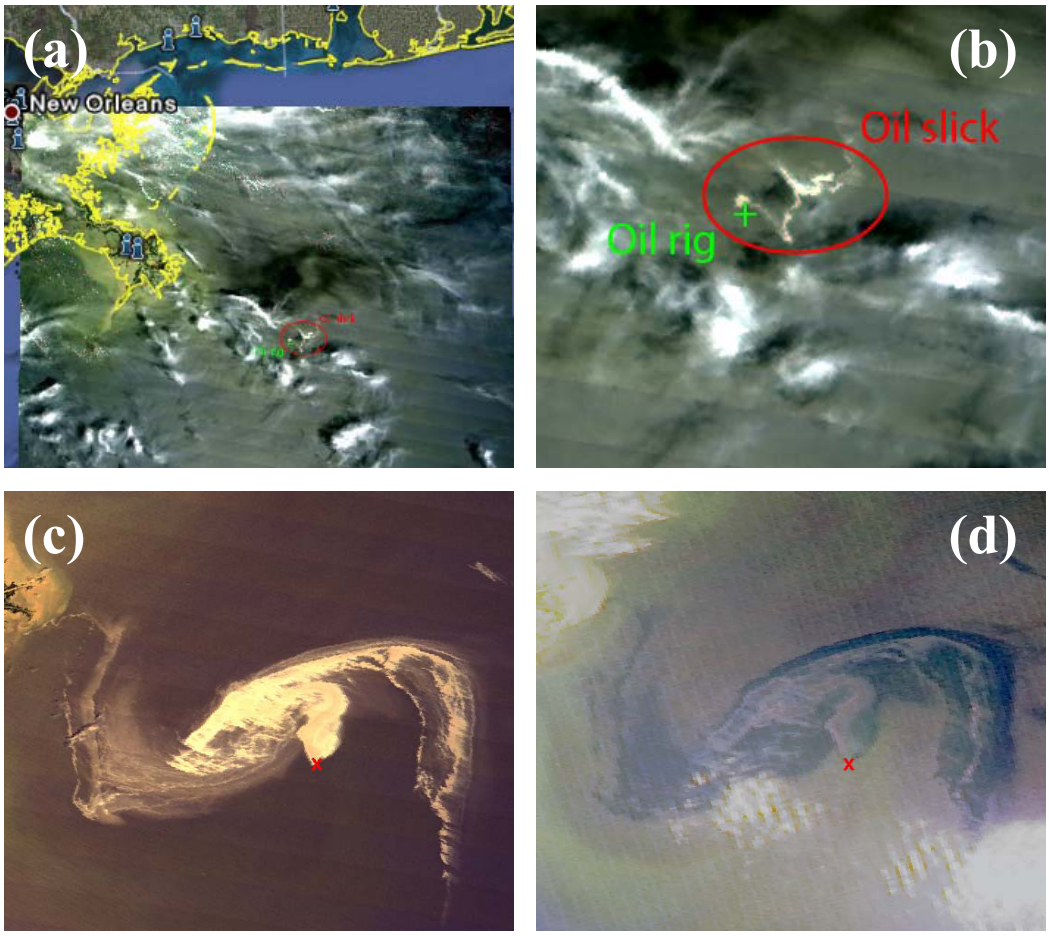

Figure 2.5 MODIS images showing oil slicks in the northern Gulf of Mexico due to oil spills from a sunken oil rig (the Deepwater Horizon) on 20 April 2010. The location of the oil rig is marked with a cross. (a) MODIS image on 22 April 2010 overlaid on a Google-Earth map shows that the oil rig is approximately 40 km southwest of the Mississippi River mouth near New Orleans, Louisiana, U.S.A. (b) An enlarged image shows the oil slick and the surrounding clouds. (c) MODIS image on 29 April 2010 (16:55 GMT) shows the oil slicks in positive contrast. (d) MODIS image on the same day but at 18:30 GMT shows the same oil slicks in negative contrast. The horizontal scale of (b)-(d) is about 120 km. More images are available at http://optics.marine.usf.edu/events/GOM_rigfire.

2.3 Training and Questions

Three MODIS RGB images are provided on the IOCCG website (http://www.ioccg.org/handbook/Hu_oil/) to help identify oil slicks and oil-like features. The first two cover the GOM, collected on 13 and 24 May 2001 by MODIS-Terra. The third image covers the ECS (25 to 35°N, 120 to 130°E), collected by MODIS-Aqua on 18 July 2008. The visualization and analysis can be performed in the following steps. We use

ENVI to describe the steps, but any other software package that has basic image processing capabilities can also be used.

1. Open the two MODIS images in ENVI. Use the "Tools → Link → Link Displays" to link the two images, so that they both show the identical region at the same time. By clicking on one image and toggling "on-off", the other image is co-registered and shown on top of the current image. This way, it is easy to identify whether certain features on the two images originate from the same locations;
2. Move the image window to the NW GOM, and use the Gaussian enhancement to enhance the colour contrast. Repeat this until a satisfactory enhanced image is obtained. This step should result in two images similar to those shown in Figure 2.4.

The second exercise is to explore the MODIS image covering the ECS. Using the interactive Gaussian stretch in ENVI, a colour-enhanced image should be obtained to show dark slicks and patches near the Yangtze River estuary in the sun glint region (Figure 2.6).

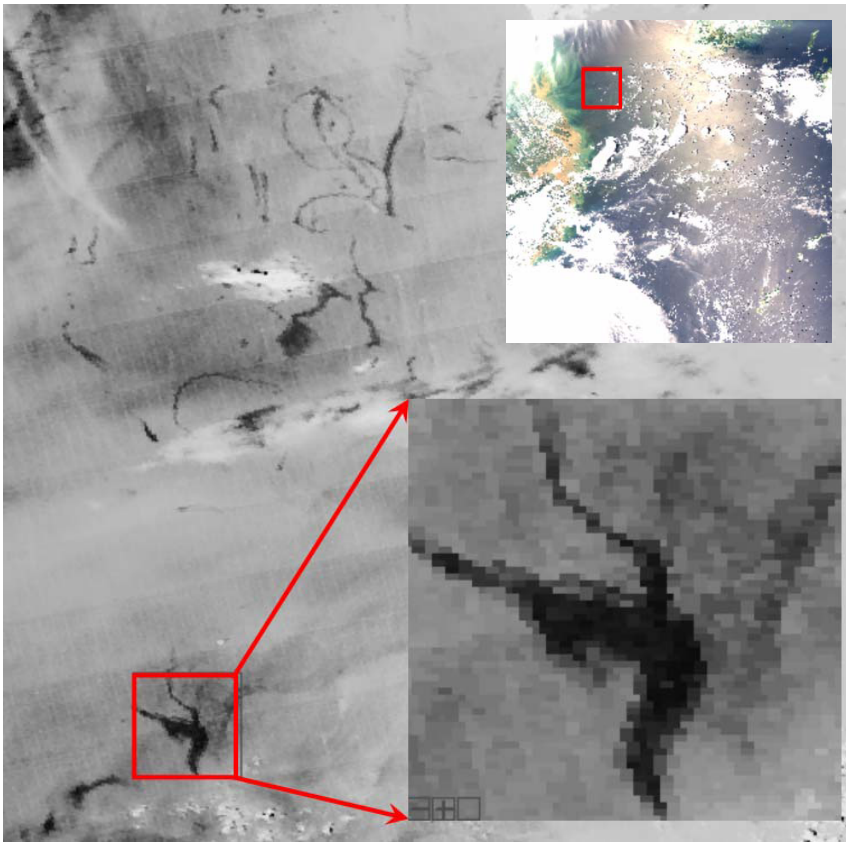

Figure 2.6 MODIS image showing surface features that appear to be oil slicks in the East China Sea (ECS). Inset: MODIS Red-Green-Blue figure covering 25 to 35°N and 120 to 130°E on 7/18/2008 04:40 GMT.

2.4 Questions

Q1: Why are the slicks brighter than the surrounding water (i.e., positive contrast) in Figure 2.4a?

Q2: Is there a one-to-one relationship between the bright slicks (Figure 2.4a) and dark slicks (Figure 2.4b), and do they have the same origins?

Q3: Are these dark features in Figure 2.6 oil films? If so, where do they come from?

2.5 Answers

A1: Crude oil from oil seeps strongly absorbs light and therefore should appear darker than the adjacent waters. Then, why are the slicks in Figure 2.4a brighter? Using MODIS data and sun-glint estimates based on solar/viewing geometry and surface wind, Hu et al. (2009) demonstrated that if the satellite views the region close to the "mirror direction" of the sun (< 12-14°), positive (i.e., brighter) contrast can result from enhanced specular reflection by the oil film. Thus, depending on how the region is viewed by the satellite (relative to the sun), the oil slicks can show no contrast (in glint-free imagery), negative contrast (low to moderate sun glint) or positive contrast (strong sun glint) in MODIS imagery. The same positive contrast is also observed in Figure 2.5a.

A2: The ENVI "Link Displays" function provides an excellent tool for tracing features on two different images. By clicking on one image with the other toggled on or off, one can easily visualize that the bright and dark slicks have a one-to-one relationship and that they indeed have the same origins. The slight difference in the traced origins between the two different days should be due to the horizontal movement during the upwelling of the bottom oil (from 1 – 2 km deep). Nevertheless, the rough locations can significantly narrow down the search range when *in situ* operations are used to locate the exact locations of the oil seeps.

A3: It is well known that the ECS, particularly the western part, is subject to oil pollution from a variety of sources, including land-based sewage discharge, illegal ship discharge, and oil transportation accidents (Li and Daler, 2004; Shi et al., 2008). Using over 600 SAR images collected over the western ECS between 2002 and 2005, Shi et al. (2008) concluded that most of the oil-like slicks were from ship discharges. The dark features shown in Figure 2.6 are from MODIS sun-glint regions, and they have spatial texture (shape, size, spatial contrast) similar to oil slicks found in MODIS sun-glint imagery in the western GOM. Therefore, in the absence of an *in situ* validation effort, and considering their proximity to the shipping routes, we can conclude that these dark features are very likely oil slicks from ship discharge. Note

that without background information or *a priori* knowledge of the study region, the difficulty in recognizing oil slicks from suspicious features also holds true for SAR imagery (Alpers and Espedal, 2004). In this regard, the performance of the MODIS sun-glint imagery in detecting oil slicks is comparable to that of SAR, except that MODIS has a lower resolution (250-m versus 25 or 10-m for SAR) and is restricted by clouds.

2.6 Discussion and Summary

The three case studies demonstrated here (one for natural oil seeps in the western GOM, one for a tragic oil spill event in the eastern GOM, and one for ship or river discharges in the western ECS) clearly show the potential of MODIS imagery in detecting oil slicks in both oligotrophic and turbid ocean waters. In turbid coastal waters where water reflectance is high, observation of oil slicks does not require sun glint, as shown by Hu et al. (2003) for Lake Maracaibo, Venezuela. Likewise, when surface oil slicks are thick, sun glint is not required either (Figure 2.5d). However, such potential of MODIS should not be over-emphasized compared with other means (e.g., SAR detection) because 1) the MODIS visible and near-IR bands cannot penetrate clouds, and the method is useless for cloud contaminated image pixels; and 2) for oligotrophic oceans and thin slicks, some degree of sun glint is required to detect the changes in surface roughness, and this requirement limits its use in high latitude regions. Finally, when sun glint is required for the observations, all limitations that apply to SAR applications for oil detection (e.g., optimal wind speed, difficulty in differentiating the various dark features) may also apply to MODIS imagery because they are based on the same principles (i.e., changes in surface roughness).

However, MODIS has the advantage of greater coverage and no data cost, thus enabling a potentially quasi-operational system to be implemented for routine applications, and fast response in case of oil spill events. MODIS has a swath width of about 2300 km, and the two MODIS instruments onboard the Terra (morning pass) and Aqua (afternoon pass) satellites make the spatial/temporal coverage at moderate resolution (250-m) unprecedented by any in-orbit satellite instruments. In this regard, for regions with a potential for heavy oil spills, a MODIS-based system could be implemented. Indeed, the most recent oil spill event in the Gulf of Mexico (Figure 2.5) provides an excellent example as to how a MODIS-based, quasi-operational system can contribute to monitoring and mitigation of oil spills. MODIS provided near daily oil spill coverage for most of the NE GOM during the first month of the spill event (21 April to late May 2010). When cloud cover increased from late May towards the summer, SAR data from several sources were combined with MODIS observations to improve the coverage. The advantage of combining more synoptic and frequent MODIS data with cloud-free SAR data in oil spill monitoring has been clearly demonstrated in this case.

In summary, oil films on the sea surface modulate the surface roughness (capillary/gravity waves), and thus can be differentiated from their surrounding waters in MODIS sun glint imagery. This ability is demonstrated by three case studies where oil slicks from natural seeps, an oil spill accident, and possible ship discharges are identified. When oil films are thick, their optical properties (light absorption and surface Fresnel reflection) can make them well distinguished from the surrounding waters, as shown in the recent GOM oil spill case study. Because of the free availability of the MODIS 250-m data since 2000, a monitoring system at low cost can be established, in principle, for any part of the global oceans where sun glint is frequently observed. Combined with SAR observations, such a system may significantly enhance our capability to monitor oil spills in most of the global oceans. Automated delineation and quantification of oil slicks (e.g., thickness) using texture analysis as well as image segmentation, however, still requires further research.

2.7 References

Alpers W, Espedal HA (2004) Oils and surfactants. In: Jackson CR and Apel JR (eds) Synthetic Aperture Radar Marine User's Manual. U.S. Department of Commerce, Washington, DC, September 2004. pp 263-275

Brekke C, Solberg AHS (2005) Oil spill detection by satellite remote sensing. Remote Sen Environ 95:1-13

Chust G, Sagarminaga Y (2007) The multi-angle view of MISR detects oil slicks under sun glitter conditions. Remote Sens Environ 107:232-239

Esaias WE, Abbott MR, Barton I, Brown OB, Campbell JW, Carder KL, et al. (1998) An overview of MODIS capabilities for ocean science observations IEEE Trans. Geosci Remote Sens 36:1250-1265

Fingas M, Brown C (1997) Remote sensing of oil spills. Sea Technology 38:37-46

Fingas M, Brown C (2000) Oil-spill remote sensing - An update. Sea Technol 41:21-26

Hu C, Li X, Pichel WG, Muller-Karger FE (2009) Detection of natural oil slicks in the NW Gulf of Mexico using MODIS imagery. Geophys Res Lett 36: L01604, doi:10.1029/2008GL036119

Hu C, Muller-Karger FE, Taylor CJ, Myhre D, Murch B, Odriozola AL, Godoy G (2003) MODIS detects oil spills in Lake Maracaibo, Venezuela. EOS, Transactions, AGU, 84(33):313,319

Li D, Daler D (2004) Ocean pollution from land-based sources: East China Sea, China. ABBIO, 33:107-113

MacDonald IR, Guinasso NL, Ackleson SG, Amos JF, Duckworth R, Sassen R, Brooks JM (1993) Natural oil slicks in the Gulf of Mexico visible from space. J Geophys Res 98(C9):16,351-16364

MacDonald IR, Reilly JF, Best SE, Venkataramaiah R, Sassen R, Guinasso N, Amos J (1996) Remote sensing inventory of active oil seeps and chemosynthetic communities in the northern Gulf of Mexico. In: Schumacher D, and Abrams MA (eds) Hydrocarbon migration and its near-surface expression. Am Assoc Petrol Geol Mem. 66:27-37

McClain CR, Feldman GC, Hooker SB (2004) An overview of the SeaWiFS project and strategies for producing a climate research quality global ocean bio-optical time series. Deep-Sea Res II 51:5-42

NAS (2003) Oil in the sea III. Committee on Oil in the Sea: Inputs, Fates, and Effects, Ocean Studies Board and Marine Board, Divisions of Earth and Life Studies and Transportation Research Board, National Research Council. The National Academies Press.

Shi LA, Ivanov YU, He M, Zhao C (2008) Oil spill mapping in the western part of the East China Sea using synthetic aperture radar imagery. Int J Remote Sens 29:6315-6329